Transactions, SMiRT-23
Manchester, United Kingdom - August 10-14, 2015
Division V, Paper ID 644

A Comparison of the Numerical Simulation of Fatigue Crack Growth in Standard Cylindrical Specimens with Experimental Values from Fatigue Endurance Testing of Nuclear Plant Materials

Jonathan Mann [1], Marius Twite [2], Chris Watson [3] and Grace Burke[4]

[1] Engineering Doctorate Student, The University of Manchester, UK
[2] Materials Technologist, Rolls-Royce, UK
[3] Principal Engineer, Rolls-Royce, UK
[4] Director, Materials Performance Centre, The University of Manchester, UK

ABSTRACT

The American Society of Mechanical Engineers Section III method for the evaluation of fatigue in nuclear plant components uses a design fatigue curve derived primarily from testing of standard smooth cylindrical specimens to describe the fatigue endurance of austenitic stainless steel material. To enable an improved understanding of the relationship between fatigue endurance results from specimens tested to a defined crack depth and the nucleation and growth of fatigue cracks in plant components, it is necessary to identify the rates of crack growth during different stages of cracking in standard endurance specimens.

In this paper numerical methods are used to quantify the fatigue crack growth between a crack depth of 0.25 mm and the depth associated with a 25% load drop in a standard cylindrical specimen (3 mm). The numerical predictions were compared with striation spacings measured at a range of crack depths on the fracture surface of an austenitic stainless steel specimen tested in air. Striation spacings were measured with a Keyence laser confocal microscope using a method described in this paper. A good correlation between numerical predictions and the measured striation spacings was obtained. Based upon the methods developed in this paper an example of an alternative best fit curve, upon which a design fatigue curve could be based, using a crack depth of 0.25 mm as the definition of crack initiation is presented.

INTRODUCTION

In order to anticipate fatigue failure in Light Water Reactor (LWR) components, fatigue life endurance assessments are conducted to verify the safe operation of plant. Within industry, these assessments are most commonly performed in accordance with an established design code such as the ASME Boiler and Pressure Vessel Codes (BPVC). For ASME grade materials, guidelines for performing fatigue life assessments are provided within Section III of the ASME BPVC, more specifically sections NB-3200, Design by Analysis and NB-3600, Piping Design, both in ASME (2013). These assessments use design data developed from the strain-controlled fatigue endurance testing of small scale metal specimens in an air environment, and are intended to give conservative fatigue lifetime assessments. In recent times evidence from a number of different studies has shown that fatigue lifetimes may be greatly reduced when a component is operated in an environment other than air, such as those encountered in LWR's as described by Chopra (1999). This in turn has led to the development of new fatigue assessment procedures to complement the ASME code methodology, such as NUREG/CR-6909 developed by Chopra and Shack (2007).

However, a problem exists in that plant operator experience seems to be at odds with the predicted reductions in fatigue lifetime associated with operation in a LWR environment, with significantly fewer

component failures and less fatigue related damage (e.g. cracking) being reported compared to what might be inferred by predictions made using the NUREG/CR-6909 methodology. It has been postulated that the discrepancy between the expected fatigue lifetimes and those observed during operation may come about as a result of significant conservatism within one or both of the ASME and NUREG/CR-6909 code methodologies.

In order to better understand any potential sources of conservatism, a study has been carried out to investigate crack growth behaviour in fatigue test specimens by means of finite element modelling. The study aims to develop bespoke relationships for fatigue crack growth in cylindrical specimens based on the results of finite element analyses and microscopy measurements on fatigued specimens. These relationships will then be used to develop the current understanding of the ASME code methodologies and how they relate to the different stages of fatigue crack growth by formulating an S-N curve that represents the number of cycles required to initiate a 0.25 mm deep crack.

BACKGROUND TO THE ASME METHODOLOGY

Fatigue design assessments are based on the use of laboratory derived S-N curves, material specific graphs relating stress or strain amplitudes to an expected number of endurance cycles for a component witnessing a similar load. S-N curves are based on the results of multiple fatigue experiments on small scale specimens, in which a specimen similar to that shown in figure 1 is repeatedly cyclically loaded at either a constant stress or strain amplitude, until a pre-defined failure criterion is met. The ASME PBVC Section III S-N curves are derived from strain controlled fatigue testing, primarily of cylindrical specimens, with failure defined as the number of cycles required to produce a 25% drop in the applied load, Watson (2011). For the diameter of specimen that was used to derive the test results, this load drop equates to a crack of approximately 3 mm in depth. Factors are applied to derive the design curves from a best fit to test data. The results are most commonly presented in terms of number of cycles to failure versus a pseudo-stress amplitude calculated from the strain amplitude and Young's modulus of the material.

A basic assumption of the ASME III methodology is that small cracks (e.g. up to a depth of 3 mm) in a cylindrical test specimen initiate and grow at the same rate as in a pressure vessel component when both are subjected to the same cyclic surface strain range. This similitude holds true for fatigue crack initiation (to achieve a defined, small crack depth), but in many cases with continued cycling this equality is not maintained. The assumption depends upon the immediate sub-surface conditions into which the crack grows. If the crack enters a decreasing stress field then more cycles will be required for the crack to grow to a pre-defined length than for a stress field that is uniform. For components with high surface strain gradients, such as those induced by the thermal shock transients that are typical of a PWR nuclear plant, conventional S-N based assessment methods such as ASME III may be overly conservative. To concede failure of a component, or even the presence of a 3 mm deep crack, based upon this type of assessment is typically unduly conservative, and for many cases the component will have a significant remnant life. In engineering terms the fatigue life of a component can be conveniently split into two phases: initiation and propagation. Initiation represents the number of cycles (N_i) to form a mechanically small crack. For the purpose of this paper, a reasonable assumption of a mechanically small crack is considered to be a depth of 0.25 mm.

There is some argument within ASME and in the wider engineering industry with regards to how the ASME failure criteria translate to real world applications, with interpretations of what is represented by the BPVC failure criteria ranging from the initiation of a crack of detectable length, to the development of a through wall leak in a component. The position within the United Kingdom is laid out by the TAGSI sub-group NT-23 who suggest that a 25% load drop represents the initiation of a crack of 3 mm depth,

Webster *et al* (2012). This is consistent with the assumption of 25% load drop in a fatigue test specimen equating to a 3 mm deep crack as stated in NUREG/CR-6909, Chopra and Shack (2007).

FINITE ELEMENT MODELLING

Various different approaches exist for modelling the growth of fatigue cracks, the two most widely used being the stress intensity factor, K, for linear-elastic crack growth, and the J-integral for elastic-plastic growth. Both methods require knowledge of the variation of these parameters with respect to the development of the crack. Standard fatigue endurance specimens representative of the type currently being used within a Rolls-Royce sponsored environmental fatigue test program at AMEC Foster Wheeler were modelled in ABAQUS in order to develop relationships for the maximum K and J values with respect to crack depth, *a*. The testing program uses displacement controlled loading to maintain a constant strain amplitude in the specimen gauge length. Testing was performed at a load ratio of R = -1. Specimens were manufactured from a 304L austenitic stainless steel and were designed in accordance with the guidelines set out in ASTM E606/E606M-12, ASTM (2012). The precise geometry of these components is shown in figure 1.

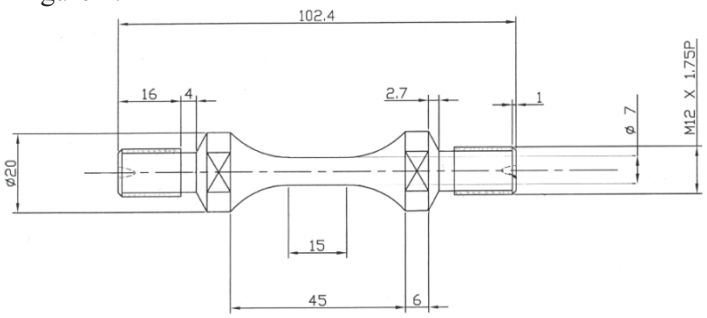

Figure 1. Schematic representation of the studied fatigue test specimen

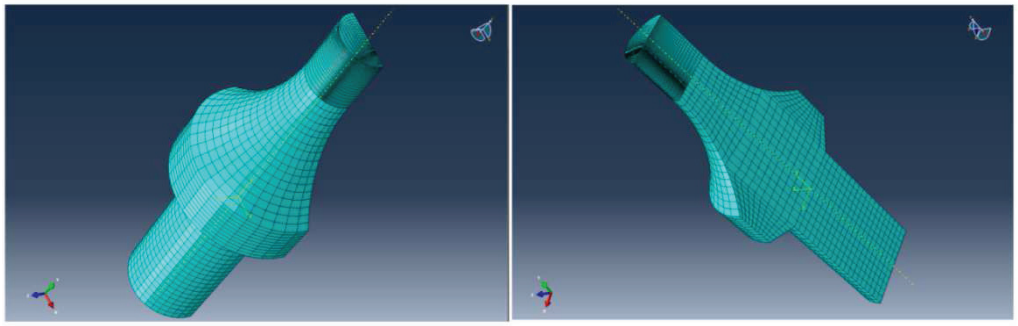

Figure 2. Finite element model of fatigue test specimen

In order to reduce computational time, advantage was taken of the problem's inherent symmetry in both the longitudinal and transverse directions by specifying symmetry conditions in both of these planes. Displacement controlled loading was applied by means of placing displacement boundary conditions on the surface of the specimen onto the areas representing the screw threads. Additional constraints, restraining both rotational and lateral movements, were placed on the screw thread surface in order to better represent the real life mechanical constraints placed upon the specimen by the test rig and to minimise any artificial bending effects. Linear-elastic analyses used a Young's modulus, E, of 195 GPa and a Poisson's ratio, ν, of 0.31. For the elastic-plastic analyses, a Ramberg-Osgood relationship derived from stabilised cyclic data of the material was used.

The models were meshed with C3D20R hex-type elements, 20-node quadratic bricks with reduced integration and are shown in figure 2. A focused mesh was used in the area immediately surrounding the

crack tip in order to increase accuracy and reduce computational requirements. For determining K and J values, 10 line contour integrals were found to give convergent solutions and results were taken from the average value reported in contours 6-10. The results for the stress intensity factor are the K_I stress intensity factors using the maximum tangential stress criterion to determine the crack growth extension direction. Cracks were assumed to have a semi-elliptical shape with an aspect ratio a/c defined as shown in figure 3. The crack aspect ratio was assumed to stay constant throughout the entirety of crack growth.

A range of finite element models based on the assumptions stated above were created containing a number of cracks between 0.2 mm and 6 mm deep. For the linear elastic modelling, a constant displacement of 0.02 mm was applied as a boundary condition which corresponded to a maximum applied strain of 0.1% (stress amplitude, σ_a = 195 Mpa) in the un-cracked specimen gauge length.

Modelling assumed that crack initiation occurred at the specimen surface. This is reasonable as results from strain controlled endurance tests at R = -1 confirm that fatigue crack initiation occurs almost exclusively at the surface in 304L austenitic stainless steel specimens. To date, it had not been possible to determine a proper crack aspect ratio from the post-test fractographic analysis of specimens. For the linear-elastic study, a crack aspect ratio of a/c=0.8 was chosen based on the observations of Findley *et al*. (2007). For the elastic-plastic analyses a/c values of 0.5, 0.8 and 1.0 were investigated in order to determine the variation in J-integral values with different crack aspect ratios.

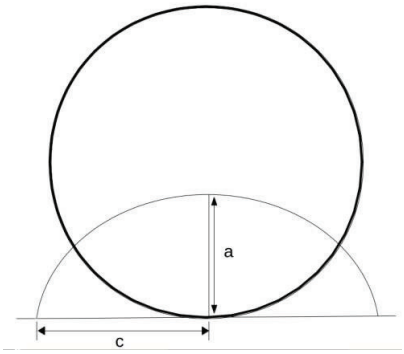

Figure 3. Assumed crack aspect ratio geometry

FINITE ELEMENT RESULTS

For each model, either the maximum K or J value associated with the maximum applied strain was reported. Figure 4 shows the results of the linear elastic analysis for a strain amplitude of 0.1% and an example of the J-integral results obtained for a strain amplitude of 0.3%. In reporting the results, both K and J values were measured along the centreline of the model in order to allow for comparison with striation counts. For the linear-elastic study, a linear increase is observed in the maximum stress intensity factor along the majority of the specimen, with a reduction in the rate of increase just prior to the onset of final fracture. The elastic-plastic profiles show an initial exponential increase in J, followed by a plateau region where the J values remain relatively constant. This is followed by a rapid increase in the value of J just prior to the onset of final fracture.

The results of the linear-elastic study were normalised in terms of the pseudo-stress in order to allow for conversion to different values in subsequent crack growth calculations using:

$$K^* = \frac{K}{\sigma\sqrt{\pi a}} \tag{1}$$

where K* is the normalised stress intensity factor and σ is the pseudo-stress obtained by $\sigma = E.\varepsilon_a$, where ε_a is the strain amplitude. The results of the elastic-plastic study are not able to be directly correlated to other strain amplitudes and subsequent crack growth analyses made direct use of the obtained J-integral profiles.

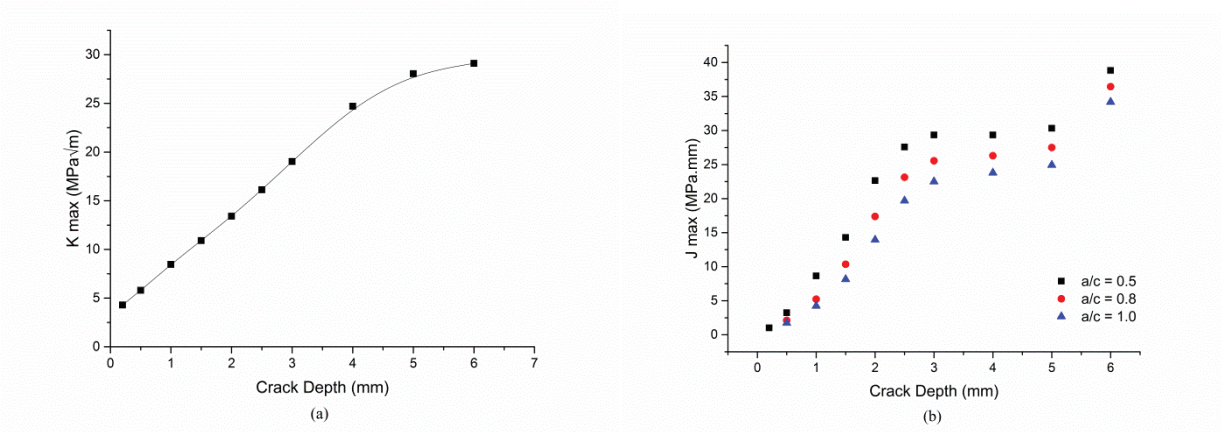

Figure 4. Finite element results. (a) Variation of stress intensity factor with crack length, $\varepsilon_a = 0.1\%$. (b) Variation of J-integral with crack length, $\varepsilon_a = 0.3\%$.

STRIATION COUNTING METHODOLOGY

Striations are characteristic features of fatigue crack growth and appear as straight, finely spaced parallel markings on fatigue fracture surfaces. A number of researchers have offered experimental evidence to suggest that the spacing of striations can be directly correlated to the fatigue crack growth rate under the assumption that one complete loading cycle leads to the production of a single striation, Connors (1994). In order to verify the results of crack growth modelling, striation counting was performed on a range of austenitic stainless steel fatigue samples. These samples were tested in air at room temperature, under displacement control, using R = -1, and at strain amplitudes of 0.2%, 0.3% and 0.6%. Two samples from tests at each strain amplitude were studied. Striation counting was predominantly performed using a Keyence VK-X200 laser scanning confocal microscope system. The system was used to create high resolution maps of the entire fracture surface in order to allow for the accurate determination of striation locations in relation to the overall crack progression. An FEI QUANTA-650 Field Emission Gun (FEG) Scanning Electron Microscope (SEM) was also used to determine the spacing of finer striations at smaller crack depths due to its improved resolution at higher magnifications. A comparison of images from the two methods is shown in figure 5 for widely spaced striations.

In order to determine the striation spacing and hence the associated da/dN, a known length of line was applied to the image in a direction perpendicular to the striations, and the number of striations intersecting that line was counted to allow for the calculation of a mean striation spacing. Multiple measurements were made in different locations close to the centreline of each fracture surface, covering a range of crack depths. It is noted that fatigue in smooth cylindrical specimens can lead to the production of complicated fracture surfaces, due to the initiation and subsequent growth of multiple interacting cracks. Striations were only sampled along the specimen centreline, on a direct line between the primary initiation site and the location of final fracture, in order to minimise the effects of multiple crack interactions on measurements.

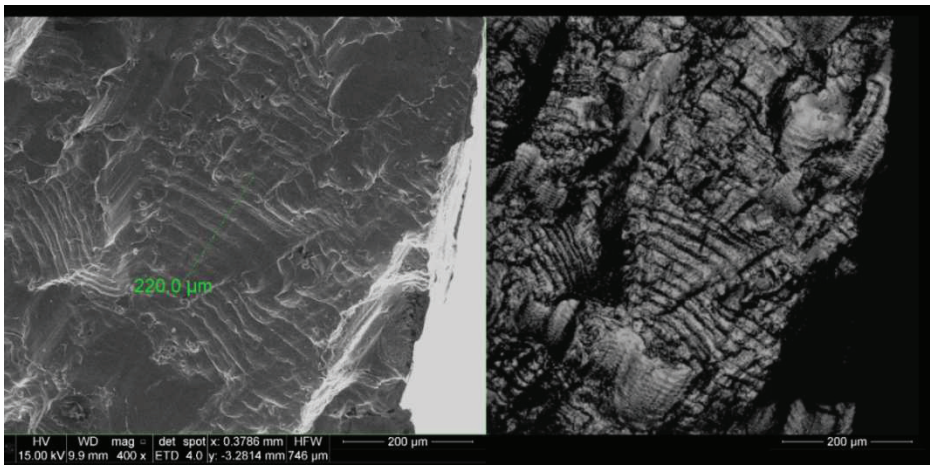

Figure 5. Comparison between SEM (left) and laser scanning confocal imaging (right) of fatigue striations

STRIATION COUNTING RESULTS

Figure 6 shows the results of the striation counting study represented in terms of mean striation spacing versus crack depth for each of the tested strain amplitudes. The striation count results revealed that under the employed test conditions, crack growth rates experience an initial exponential rise before achieving a steady crack growth rate after the crack has propagated approximately halfway across the 7 mm diameter of the specimen. This is followed by a rapid increase in the rate of crack growth just prior to final fracture. This observation corresponds well with the J-integral profiles obtained from the elastic-plastic finite element analyses.

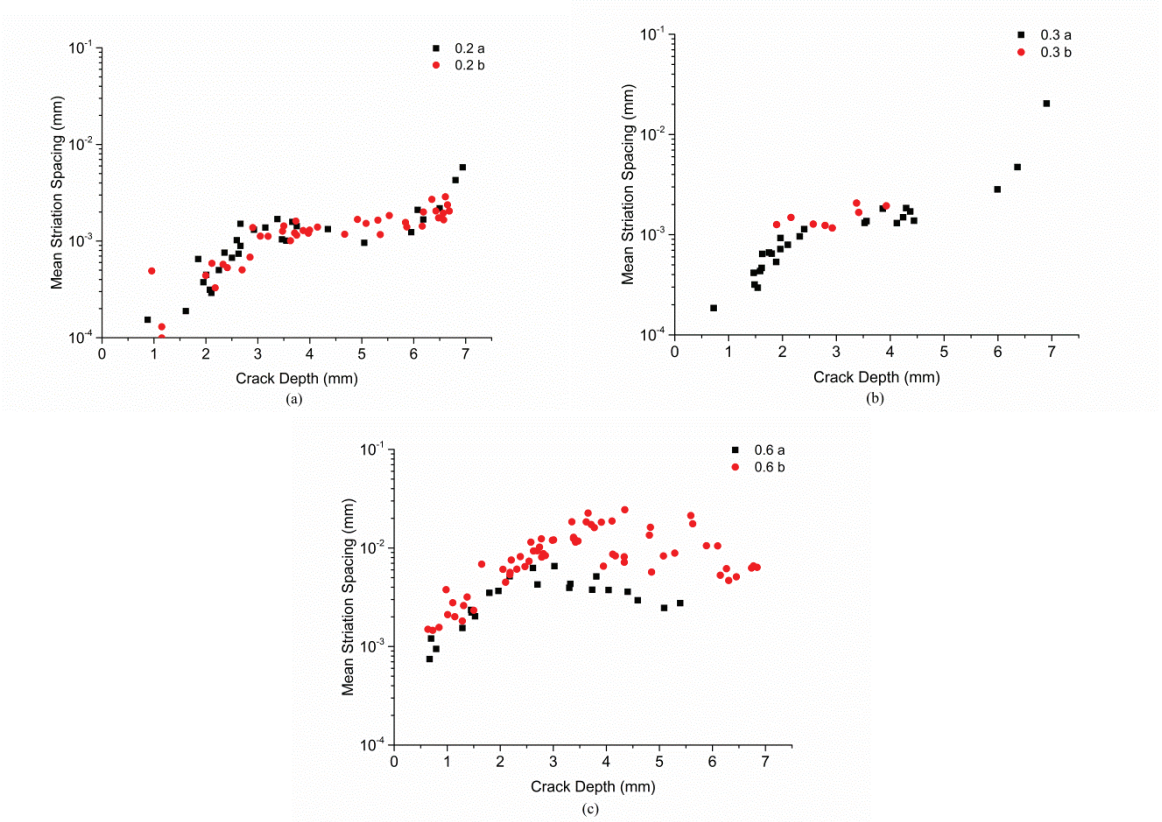

Figure 6. Results of striation counting (a) $\varepsilon_a = 0.2\%$, (b) $\varepsilon_a = 0.3\%$, (c) $\varepsilon_a = 0.6\%$

Striation counts from different specimens tested at the same intermediate strain amplitudes of 0.2 and 0.3% produced similar results in terms of striation spacing. However, the profiles obtained from tests performed at the higher strain amplitude of 0.6% showed more variation, without the same clear plateau region or large increase in J prior to fracture. This is due to the fact that at higher strain amplitudes, multiple cracks are initiated and experience some period of growth, leading to interactions between different cracks and a resulting complicated effect on crack growth rates. The crack growth rate measurements taken at lengths of less than 3 mm show reasonably good agreement with each other, and were thus assumed to properly represent the crack growth rate in this region.

FATIGUE CRACK GROWTH CALCULATION METHODS

Linear-elastic crack growth calculations were performed using the derived K_{max} versus a profile. Crack growth per cycle was determined using the ASME air crack growth law for stainless steels at room temperature, ASME (2013b). It was assumed that at strain amplitudes lower than 0.2% the material will respond in a nominally elastic manner. An effective stress intensity factor range, ΔK_{eff} was used to calculate crack growth rates, defined as:

$$\Delta K_{eff} = K_{max} + ff\, K_{max} \tag{2}$$

where ff is a crack closure factor which represents the portion of the compressive applied stress intensity factor that applies to the overall ΔK for each cycle. A study by Watson *et al.* (2015) on similar materials showed that an ff value of 0.27 represented a bound to nominally elastic behaviour and was a best fit to the nominally non elastic data. Thus, this value was chosen for the subsequent analyses.

In order to determine crack growth rates as a function of the J-integral, a ΔJ methodology was used. The ASME crack growth law was modified using a method described by McClung *et al*. (1999), whereby each ΔK value is converted into its ΔJ equivalent through:

$$\Delta J = \Delta K^2 / E' \tag{3}$$

where $E' = E/(1-\nu^2)$ for plane strain. The validity of converting ΔK based crack growth data into its ΔJ equivalent is supported by a number of previous investigators who have reported on its successful use in representing both long and short crack growth in elastic-plastic fatigue problems, Dowling (1976). The modified ASME Paris law in terms of ΔJ is thus given by:

$$\frac{da}{dN} = 1.34798 \times \Delta J^{1.65} \quad (mm/cycle) \tag{4}$$

Calculation of ΔJ is usually performed by means of approximations based on cyclic hysteresis loops. In the present study, a simplified approach based on the ΔK_{eff} method described above was attempted. The maximum J-integral values obtained from the finite element analysis were used in an equivalent manner to K_{max} in order to produce an effective ΔJ defined as:

$$\Delta J_{eff} = J_{max} + ff\, J_{max} \tag{5}$$

For an assumed crack aspect ratio of 0.5, this approach was found to give very good agreement with the results of striation counting for cracks longer than 1.5 mm depending on the chosen value of ff. As an example, figure 7a shows the results of using this method to model fatigue crack growth in one of the specimens tested at a 0.3% strain amplitude (a/c = 0.5, ff=0.27). The method is able to accurately capture the initial exponential growth at a > 1.5 mm, as well as the subsequent plateau and final increase in crack growth rates. Due to its excellent correlation with the measured striation spacing, this method was adopted for the subsequent crack growth calculations, however it is not claimed to be generally applicable to other elastic plastic fatigue problems.

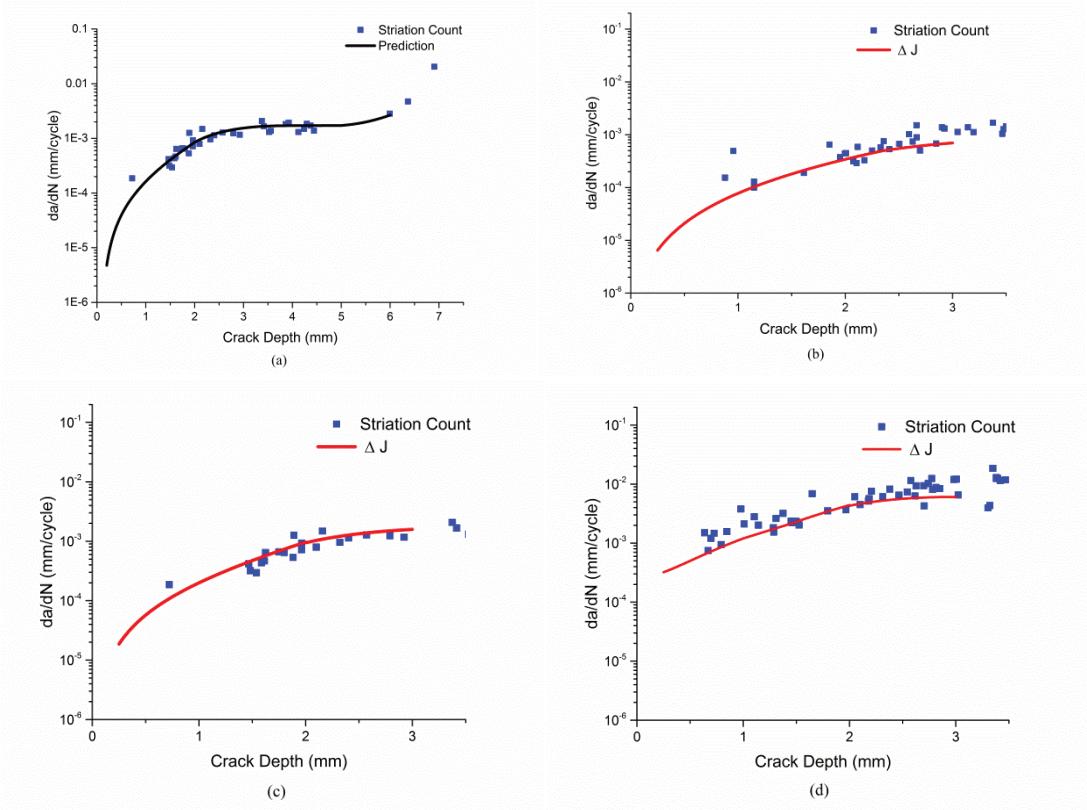

Figure 7. Elastic-plastic crack growth predictions. (a/c = 0.5, ff = 0.27)
(a) Example $\varepsilon_a = 0.3\%$ profile. (b) $\varepsilon_a = 0.2\%$, $a_0 = 0.1$mm.
(c) $\varepsilon_a = 0.3\%$, $a_0 = 0.1$mm. (d) $\varepsilon_a = 0.6\%$, $a_0 = 0.1$mm.

For both the linear-elastic and elastic-plastic analyses, growth rates for smaller cracks (a < 1.5 mm) were severely under-predicted when compared to the results of the striation counts. This behaviour has been noted by many previous researchers and is commonly referred to as the 'short crack problem'. In order to account for this, an effective crack length, a_{eff}, (where $a_{eff} = a + a_0$) was used in the crack growth calculations, El Haddad *et al.* (1980). a_0 is a material parameter which accounts for the non-continuum behaviour of very small cracks. a_0 is given by:

$$a_0 = \left(\frac{\Delta K_{th}}{\Delta \sigma_e}\right)^2 \frac{1}{\pi} \tag{6}$$

where ΔK_{th} is the threshold stress intensity factor range and $\Delta\sigma_e$ is the endurance strength range of the material. a_0 was estimated to be approximately equal to 0.1 mm. The addition of an effective crack length produced a closer fit to the striation count data for shorter cracks and the resulting growth profiles agreed well with the lower bound of the striation count data for ff = 0.27 (Figures 7 b-d). This value was chosen due to the fact that it represented the lower end of the experimental data well. The chosen method tends towards over-predicting the number of growth cycles, which increases conservatism in the results when attempting to subsequently back-fit the ASME curve.

DERIVATION OF BEST-FIT FATIGUE CURVE CORRESPONDING TO A 0.25 mm CRACK

The established crack growth expressions were used to determine the number of cycles necessary to grow a crack from 0.25 to 3 mm, the latter crack depth being assumed to correspond to the 25% drop in load used as the failure criterion in NUREG/CR-6909 and the ASME design fatigue curves. The calculated number of cycles was then subtracted from the corresponding fatigue life, as given by the NUREG/CR-

6909 best fit curve for austenitic stainless steels in air, in order to produce a curve that estimates the number of cycles required to initiate a 0.25 mm deep crack (figure 8).

This new curve could be used to improve estimates of fatigue life of LWR plant components by using the curve to estimate the number of cycles required to initiate a fatigue crack and grow this to 0.25mm depth, which could be followed by a fatigue crack growth analysis based on da/dN vs. ΔK laws derived from test results gained from pre-cracked compact tension specimens; such laws are available in the ASME BPVC Section XI. The advantage of this approach would be the elimination of the element of fatigue crack growth between 0.25 mm and 3 mm crack depths that is included in the NUREG/CR-6909 best fit to fatigue endurance data. This is due to the fact that within this crack depth range, the associated period of crack growth in a fatigue test specimen may not represent growth to 3 mm depth in a component due to the observed complex variation in crack growth rate as a crack grows through a small specimen. The 0.25 mm best fit curve could also be factored to provide a design curve, in the same way as is done for the 3 mm best fit curve in NUREG/CR-6909.

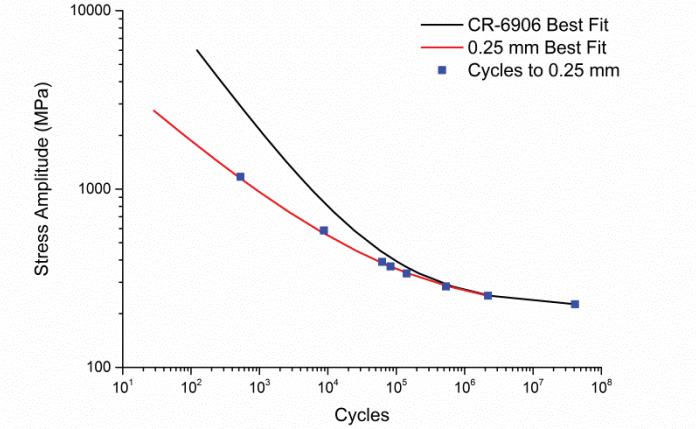

Figure 8. Back-fitting of the ASME fatigue curve in order to produce an equivalent 0.25 mm initiation best fit curve

CONCLUSIONS

Discrepancies between the fatigue predictions produced by established engineering standards and the relatively low amount of failures and damage reported by industry highlight the need to develop a better understanding of how these standards apply to real life components. The separation of the fatigue life into separate parts (i.e. crack nucleation, crack growth to a defined short depth, and the subsequent growth of longer cracks) could help to produce more accurate representations of the progression of fatigue damage under non-standard loading conditions, such as when a crack grows into a decreasing stress field. In this paper, a curve estimating the fatigue lives of austenitic stainless steel specimens to a crack depth of 0.25 mm has been produced from the NUREG/CR-6909 best fit data using crack growth predicted from finite element modelling of the specimen design. Future studies should aim to provide additional verification of the presented methodology by investigating the striation spacing on specimens tested at both higher and lower strain amplitudes than those that were included in the current study.

Striation counts taken from the fracture surfaces of failed austenitic stainless steels components showed a good correlation with predicted crack growth rates when a > 1mm, suggesting that for this material each individual striation can be assumed to represent one full loading cycle. A simplified ΔJ approach was shown to be effective in characterising fatigue crack growth rates depending on an assumed contribution of compressive J. Despite showing excellent correlation with the measured data, this technique is not theoretically validated and further work would be needed in order to properly verify its usage for other applications or to apply the technique in justification of nuclear plant components.

A significant source of conservatism in the above analyses came from the treatment of short crack growth. A more in depth analysis of the crack growth rates for cracks less than 1.5 mm deep would serve to increase the accuracy of the predictions. This would include higher resolution striation counting at smaller crack depths and a more detailed investigation into different short crack growth modelling assumptions.

REFERENCES

ASME, ASME Boiler and Pressure Vessel Code, Section III, Division 1, Appendices, Mandatory Appendix 1 Design Fracture Curves (2009)

ASME, ASME Boiler & Pressure Vessel Code, Section XI, Division 1, C-8400. (2007)

ASTM Standards Volume 03.01. "Standard test method for strain-controlled fatigue testing", E606/E606M-12. (2012).

Chopra. O.K. "Effects of LWR Coolant Environments on Fatigue Design Curves of Austenitic Stainless Steels Effects of LWR Coolant Environments on Fatigue Design Curves of Austenitic Stainless Steels." Technical report, Argonne National Labs, Argonne, (1999).

Chopra, O. K., and W. J. Shack. "Effect of LWR Coolant Environments on the Fatigue Life of Reactor Materials NUREG/CR-6909." (2006).

Connors, William C. "Fatigue striation spacing analysis." *Materials characterization* 33, no. 3 (1994): 245-253.

Dowling, N. E. "Geometry effects and the J-integral approach to elastic-plastic fatigue crack growth." *Astm Stp* 601 (1976): 19-32.

El Haddad, M. H., N. E. Dowling, T. H. Topper, and K. N. Smith. "J integral applications for short fatigue cracks at notches." *International Journal of Fracture* 16, no. 1 (1980): 15-30.

Findley, K. O., S. W. Koh, and A. Saxena. "J-integral expressions for semi-elliptical cracks in round bars." *International journal of fatigue* 29, no. 5 (2007): 822-828.

McClung, R. Craig, G. G. Chell, Y-D. Lee, D. A. Russell, and G. E. Orient. "Development of a practical methodology for elastic-plastic and fully plastic fatigue crack growth." (1999).

TAGSI, "Consideration of Margins in ASME Fatigue Design Curve", The UK Technical Advisory Group on the Structural Integrity of High Integrity Plant, TAGSI/P(12)203, TAGSI/NT-23/P(12)22, June (2012).

Watson, C. T. "The Background to Light Water Reactor Environment Fatigue Evaluation Methods for Austenitic Stainless Steel and their Application to Sample Pressurised Water Reactor Components." In *ASME 2011 Pressure Vessels and Piping Conference*, pp. 539-551. American Society of Mechanical Engineers, (2011).

Watson, C. and Currie, C. "Accounting for negative R-Ratio (crack closure) in fatigue crack growth calculations on stainless steel components." *ASME 2015 Pressure Vessels and Piping Conference Proceedings*. American Society of Mechanical Engineers, (2015).